

Two-way fluid-structure interaction of medium-sized heliostats

Cite as: AIP Conference Proceedings **2126**, 030064 (2019); <https://doi.org/10.1063/1.5117576>
Published Online: 26 July 2019

Joshua R. Wolmarans, and Ken J. Craig



View Online



Export Citation

ARTICLES YOU MAY BE INTERESTED IN

[Hami - The first Stello solar field](#)

AIP Conference Proceedings **2126**, 030029 (2019); <https://doi.org/10.1063/1.5117541>

[Dynamic load mechanical modelling of a 10 MW tensile ganged heliostat prototype](#)

AIP Conference Proceedings **2126**, 060001 (2019); <https://doi.org/10.1063/1.5117587>

[From research to industry: Development of a high-resolution measurement system for mirrored heliostats in series production](#)

AIP Conference Proceedings **2126**, 030051 (2019); <https://doi.org/10.1063/1.5117563>

Lock-in Amplifiers
up to 600 MHz



Two-Way Fluid-Structure Interaction of Medium-Sized Heliostats

Joshua R. Wolmarans¹ and Ken J. Craig^{2, a)}

¹Graduate student, Department of Mechanical and Aeronautical Engineering, University of Pretoria, Pretoria 0002, South Africa.

²PrEng, PhD, Professor, Department of Mechanical and Aeronautical Engineering, University of Pretoria, Pretoria 0002, South Africa.

^{a)}Corresponding author: ken.craig@up.ac.za

Abstract. Vortex shedding and the resultant transient loadings on a medium sized heliostat are investigated in this paper. Reynolds-Averaged Navier-Stokes (RANS) Computational Fluid Dynamics (CFD) is used as a validation case along with laminar and Large Eddy Simulation Fluid-Structure Interaction (FSI) validation. 2-Dimensional unsteady RANS and FSI are performed where the shedding frequency is found at the experimentally predicted Strouhal number, which is also in the region of concern as confirmed via a modal analysis of the heliostat structure. Stress-Blended Eddy Simulation (SBES) is then used as a scale-resolving method in order to accurately simulate the transient peak loading and vortex shedding in three dimensions. The SBES simulation results show that the 2D URANS results captured one of the main vortex-shedding frequencies. Initial deformation results from a transient structural analysis using the temporal SBES heliostat surface pressure fields as input indicate that the method holds promise in predicting the transient response of heliostats.

INTRODUCTION

Heliostat structures make up a large portion of the initial capital cost of a central receiver concentrating solar power plant due to the amount of heliostats needed, especially for medium-sized heliostats like the LH-2 used at Ivanpah (173 500) [1]. As can be seen in Fig.1 [2], the heliostat field can account for almost a third of the costs of a Concentrated Solar Power (CSP) tower plant. Improving the design of heliostats to be lighter, use less material and require smaller actuators would all be cost-reducing drivers. Wind loading is the main factor that may cause degradation in heliostat optical and structural performance and plant availability.

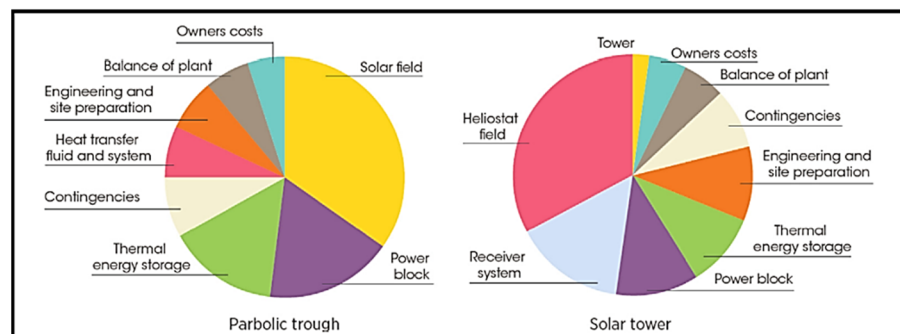


FIGURE 1. Breakdown of different CSP costs [2]

Heliostats are by nature very active pieces of hardware, their function in reflecting the sun's solar radiation requires that they constantly track the sun's position with movement about at least two axes. The angle of the mirror constantly

changes throughout the day; this leads to varying wind loads on the heliostat, and coupled with the individual heliostat's placement in the field, creates fluctuating conditions that need to be designed for. Heliostats that are located on the outer edge of the heliostat field face greater wind loads than those that are sheltered near the centre. For optimal operation the heliostats are required to be as stiff as possible, both statically and dynamically.

The fact that the heliostats have to face the natural elements, particularly wind, makes their design a highly complex task. Atmospheric Boundary Layer (ABL) modelling is needed to try and replicate the conditions experienced by the heliostats on the ground. ABL modelling is in itself a complicated area of science and numerous papers exist detailing the best approaches that should be used when modelling this in Computational Fluid Dynamics (CFD). Many factors can influence the models such as boundary and inlet conditions, and the nature of wind loading is in itself stochastic. This leads to the problem of over and under-design of the heliostats, over-design due to the poor prediction of the wind loads means that the heliostat structures are larger than they need to be and ultimately more expensive than they should be. This is the main issue that this project attempts to deal with, reduction of costs based on the optimal design. Under-design is just as much of an issue as this would lead to the inevitable failure of the heliostat before its designed lifespan, causing excessive maintenance costs and possibly the closure of an operational plant.

When refining heliostat designs, fluid-structure interaction (FSI) becomes more important and needs to be well understood to assess its affect. To reach this goal, this study proposes a two-way coupling of ANSYS Fluent CFD and ANSYS Mechanical Finite Element Analysis (FEA) on a simplified version of the LH-2 heliostat, henceforth called the "heliostat", seen in Figure 2.

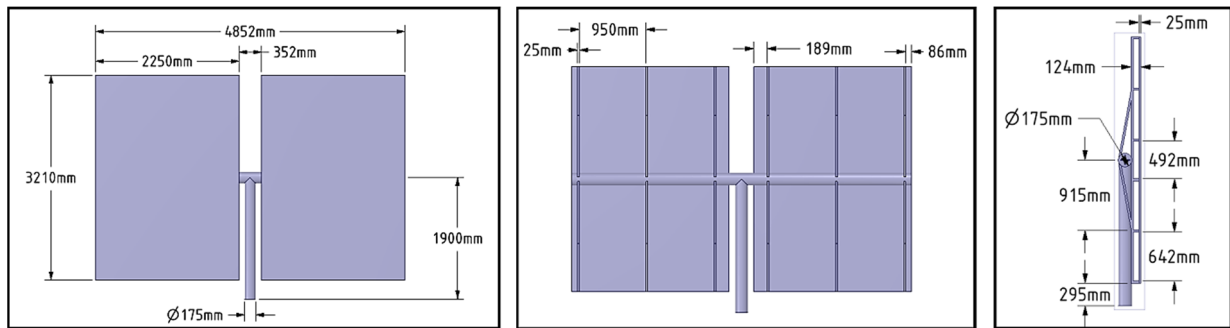


FIGURE 2. Computational model of the simplified LH-2 heliostat

METHODOLOGY

The first step in accurately modelling the flow over a heliostat is correctly characterising the ABL. Blocken et al [3] and Richards and Norris [4] provide guidelines for the correct modelling of the ABL. Blocken et al stress the need for a horizontally homogeneous ABL in the computational domain, this means that in the vertical profiles of the mean velocity and turbulence there is an absence of streamwise gradients. This will occur when the mean velocity and turbulence profiles are in equilibrium with the roughness characteristics of the ground surface [3]. Richards and Norris [4] detail certain requirements for the ABL to achieve homogeneity, the boundary conditions, turbulence models and the associated constants must be consistent. Blocken et al [3] describe four requirements that need to be simultaneously satisfied if the wall roughness is expressed by an equivalent sand grain roughness in the wall functions which is the case here. The four requirements are listed below:

1. A sufficiently high mesh resolution in the vertical direction close to the bottom of the computational domain.
2. A horizontally homogeneous ABL flow in the upstream and downstream region of the domain.
3. A distance y_p from the centre point P of the wall adjacent cell to the wall that is larger than the physical roughness height K_s of the terrain. (No longer needed due to software advances)
4. Knowing the relationship between the equivalent sand grain roughness height and the corresponding aerodynamic roughness length z_0 [3].

Once the ABL is modelled correctly, the mean flow over the heliostat can be modelled with confidence using Reynolds-Averaged Navier-Stokes (RANS) CFD, here using either the Realizable $k-\epsilon$ (RKE) and SST $k-\omega$ turbulence models. As the first step in accounting for transient effects, Unsteady RANS (URANS) is implemented in the 2D two-way Fluid Structure Interaction (FSI) as well as the 3D two-way FSI. An example of the ANSYS Workbench setup

for a two-way FSI simulation using System Coupling can be seen in Figure 3. A modal analysis is performed on the full-scale 3D heliostat in order to investigate the frequencies that may be of concern with regards to vortex shedding and transient peak loadings. To resolve peak loadings, Scale-resolving CFD is implemented using the Stress-Blended Eddy Simulation (SBES) model, a hybrid model that utilises both RANS and Large Eddy Simulation (LES) capabilities. The wall bounded flow is modelled with the SST $k-\omega$ model while the main turbulence features of the flow are resolved with LES. This is used in order to assess the peak loadings on the heliostat due to the vortex shedding which cannot be modelled using URANS. The pressure field developed on the heliostat structure is transferred to ANSYS Mechanical where a transient structural analysis is performed. In the current study, both one-way and two-way coupling are investigated using 2-D and 3-D models, with the aim of finding the most cost-effective way of determining peak loadings.

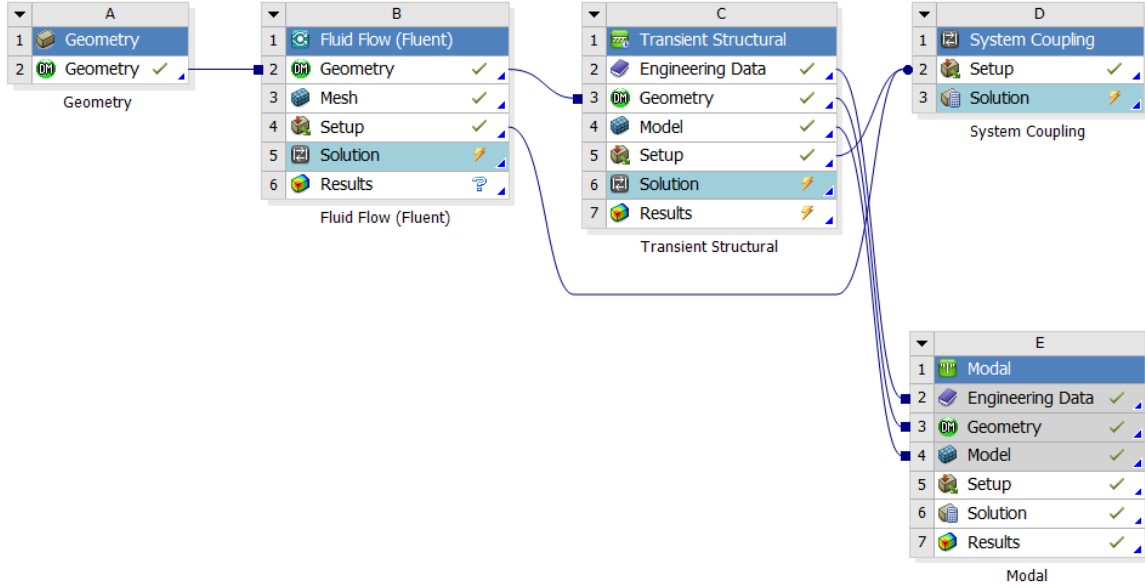


FIGURE 3. ANSYS Workbench two-way FSI simulation layout.

MODELLING THE ABL WITH RANS

The ABL was validated using the wind tunnel experiments of Peterka [7]. The inlet velocity profile and the turbulence intensity profiles of Peterka were used to find an optimal aerodynamic roughness height z_o that would allow the profiles used in the CFD to be as accurate as possible. The normalized velocity profile used can be seen in equation 1:

$$\frac{u(z)}{u_{Ref}} = \frac{\ln\left(\frac{z}{z_o}\right)}{\ln\left(\frac{z_{Ref}}{z_o}\right)} \quad (1)$$

with u_{Ref} the velocity at a reference height, z_{Ref} . The only value that can be altered to match a given velocity profile is that of the aerodynamic roughness z_o , given the information and the profiles from the Peterka study. Either an optimized z_o can be found for the inlet velocity profile using equation 2, or an optimal z_o can be determined to model the turbulence intensity profile using equation 3. The profiles for the optimized velocity profile and turbulence profiles can be seen in Fig. 4, when using equation 2 or 3, respectively. As matching the turbulence intensity profile does not influence the velocity profile matching to a large extent, it is used in the rest of the study.

$$Er(z_o) = \sum_{\eta=1}^{\xi} \left[U_{\eta} - U_{Ref} \frac{\ln\left(\frac{z}{z_o}\right)}{\ln\left(\frac{z_{Ref}}{z_o}\right)} \right]^2 \quad (2)$$

$$Er(z_o) = \sum_{\eta=1}^{\xi} \left[I_{u\eta} - \frac{\frac{\left(\frac{2}{3}\right) \left(\frac{u_{Ref}^{\kappa}}{\ln\left(\frac{z_{Ref}+z_o}{z_o}\right)} \right)^2}{(\sqrt{C_u})}}{\frac{U_{Ref} \ln\left(\frac{z}{z_o}\right)}{\ln\left(\frac{z_{Ref}}{z_o}\right)}} \right]^2 \quad (3)$$

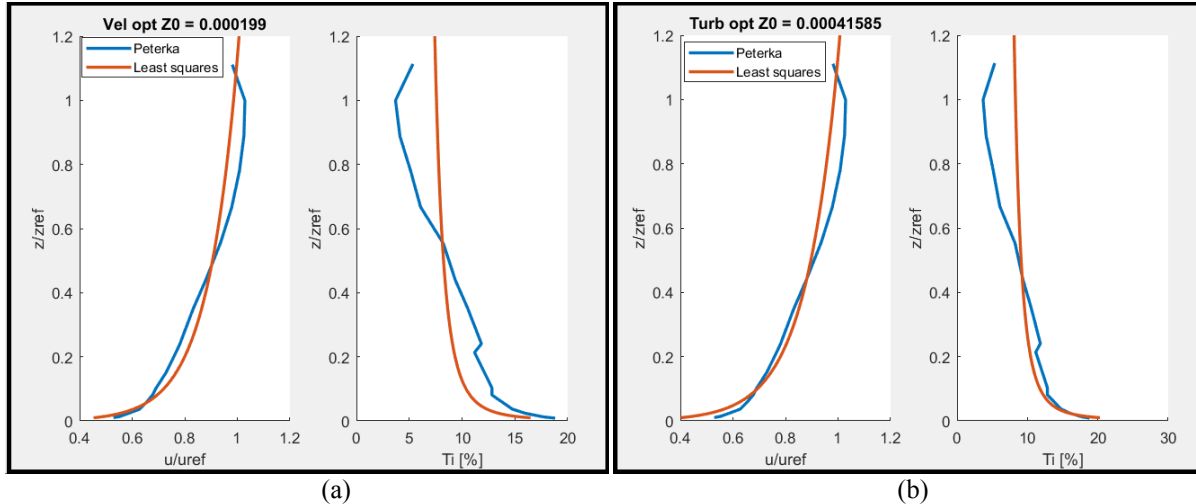


FIGURE 4. Optimized velocity and turbulence intensity profiles based on a) matching velocity, b) matching turbulence intensity.

The wind tunnel and CFD results of Huss et al [1] were used as validation of the implementation of the current RANS method (RKE). Figure 5 shows the mean drag and torque tube moment coefficients over various elevation angles. The current CFD predictions of force and moment coefficients are within 18% of the experimental bands and outperform the CFD results of [1]. The validation provides confidence in the use of RANS as precursor for scale-resolving CFD.

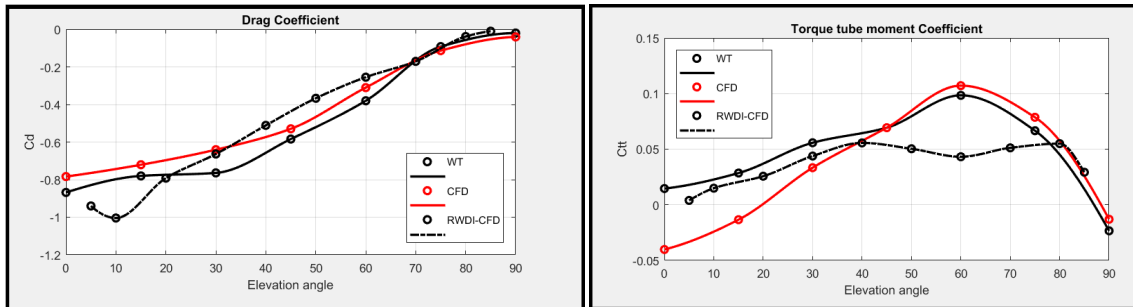


FIGURE 5. Drag and torque-tube moment coefficient validation (RWDI-CFD and WT results from [1]).

2D FLUID-STRUCTURE INTERACTION AND MODAL ANALYSIS

An FSI validation is conducted on the numerical simulations presented by Bungartz and Schäfer [5] on a flexible flap attached to a cylinder in both laminar and turbulent flow. The case makes use of a one-cell thick domain, LES is used for the turbulent validation case. The results of the FSI validation are an exact match, Figure 6a) shows the accuracy in the Fast Fourier Transform (FFT) of the FSI simulation. The FFT for the displacement of the trailing edge of the flap is an identical match to the Strouhal number provided by [5]. Velocity magnitude and pressure contours are also displayed for the laminar (Fig.6b) and turbulent case (Fig.6c)). The FSI validation performed in ANSYS Workbench with the use of System Coupling is thus successfully validated.

A Modal analysis was performed for the heliostat structure, as summarized in Figure 7. The modal frequencies obtained are in a similar range as those of Griffith et al [8]. The structural meshed model is shown in Fig.7a) along with the table of the first five modal frequencies (Fig.7b)). The modal analysis provides insight into the natural frequency ranges of the heliostat that need to be avoided during vortex shedding. A 2D two-way FSI simulation was conducted on the heliostat using SST $k-\omega$ URANS and System Coupling. The results of this simulation show that the vortex shedding attained match perfectly to the predicted results from the Matty [6] wind tunnel experiments of Strouhal numbers of the vortex shedding behind a flat plate. The velocity contour plot is shown in Fig. 7d) for the 2D

two-way FSI along with the FFT of the CFD-only drag coefficient signal (Fig.7c)). The FFT clearly shows the main frequency component of the drag due to regular vortex shedding visible in Fig.7d) as the predicted 0.5 Hz, with an additional component in the 1 Hz range and a smaller spike at around 1.5 Hz. This 1.5 Hz spike is of interest as it is in the vicinity of the first mode of the heliostat structure found in the modal analysis.

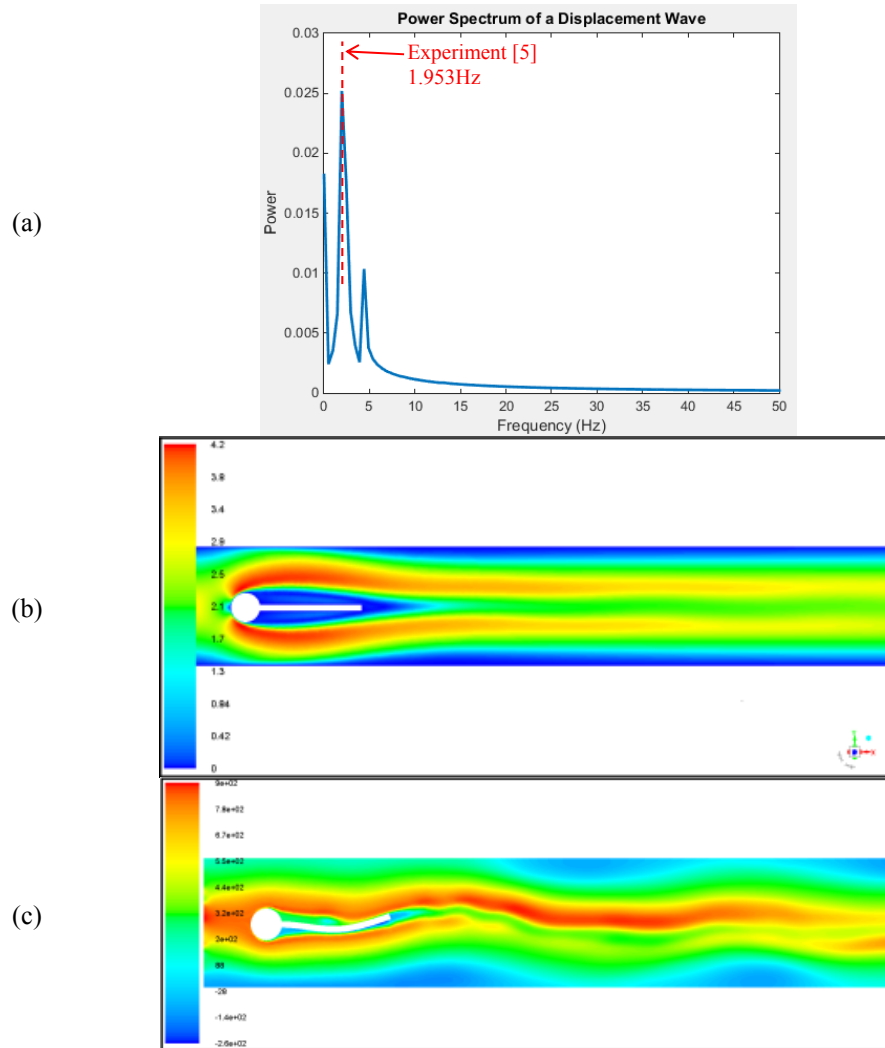


FIGURE 6. Two-way FSI validation of flexible flap. a) Power spectrum of displacement (laminar CFD, compared to results of [5], b) Velocity contours of laminar case, c) Pressure contours of turbulence case

SCALE-RESOLVING CFD AND ONE-WAY FSI

Due to the inability of URANS to model vortex shedding for this geometry in 3D (not presented here), scale-resolving CFD was used to accurately resolve the turbulent structures thus providing the transient peak loadings experienced by the heliostat. The SBES hybrid model was implemented as it allows a coarser mesh on the wall boundary flow to be employed as this is modelled with SST $k-\omega$ RANS while the LES capabilities of the SBES model are used to resolve the turbulence generated by the heliostat and introduced at the inlet of the computational domain. The SBES CFD case consists of approximately 28 million computational cells. The inlet synthetic turbulence is generated via the Vortex Method. Turbulence then is allowed to be produced and dissipated using the SBES method. At a location just upstream of the heliostat, the energy spectrum of the flow can be seen in Figure 8. The anisotropic large-scale eddies as well as the inertial subrange is resolved by LES up to subgrid-scale frequencies where the viscous

dissipation is modelled. Kolmogorov's theory predicts a slope of $-5/3$ for the inertial sub range, which is captured to a large extent as seen in Fig. 8

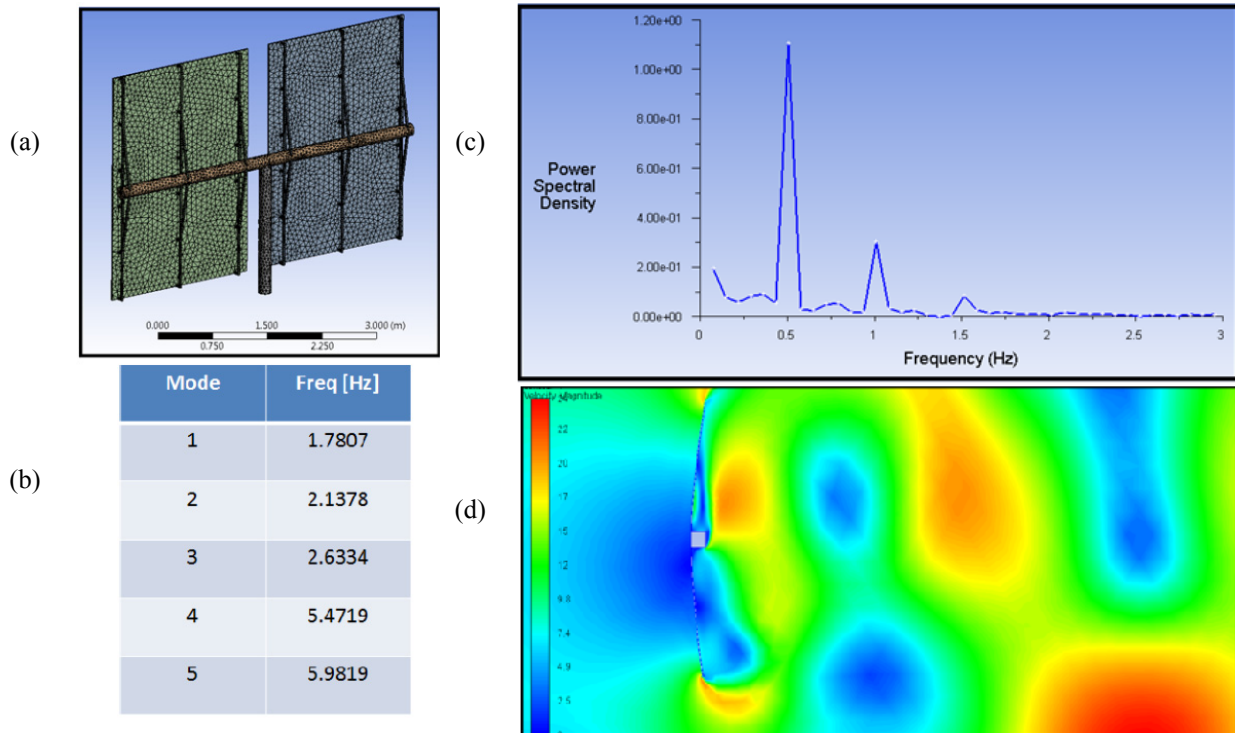


FIGURE 7. a) Heliostat structural mesh, b) first five modal frequencies, c) FFT of the 2D CFD drag coefficient signal, d) 2D two-way FSI velocity contour plot

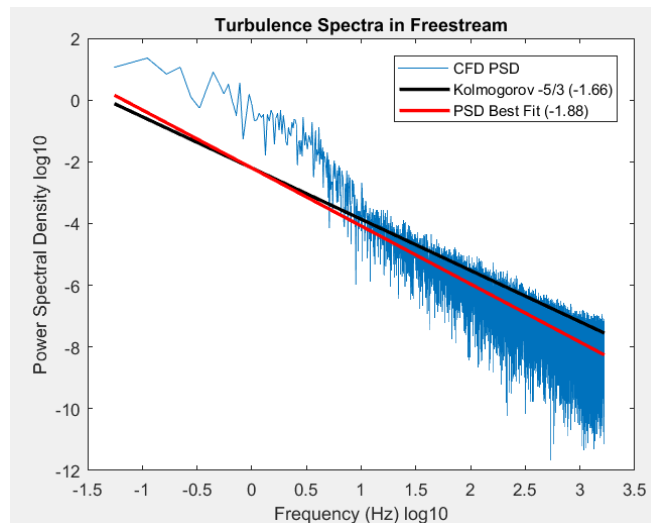


FIGURE 8. Turbulence spectrum in freestream of SBES simulation just upstream of the heliostat.

The SBES simulation is run for approximately 20 seconds with the computational domain being roughly 100m in length, this equates to $2 \times$ fluid flow throughs of the domain providing enough flow information for data statistics. The SBES simulation is conducted for both the 0° (upright) case where the drag is a maximum and for the 60° elevation angle case where the torque-tube moment is a maximum (Fig.5). The drag coefficient for both cases along with the

lift and torque tube moment for the 60° case can be seen in Figure 9. There are numerous uncharacteristic spikes in the drag and lift coefficient histories which may be due to the Vortex Method creating spurious high and low pressure cells that attack the heliostat. The comparison between the averaged SBES results and those of the experiments of Ref.1 is promising, but may point to a longer run-time being required.

The FFTs of signals of the heliostat drag coefficient and the velocity magnitude of a monitor point in the wake of the heliostat from the SBES simulation are shown in Figure 10. Both FFTs contain a strong 0.5 Hz frequency component as found in the 2D case (Fig.7c) and as predicted from the experimental results of [6] as the main shedding frequency. The frequency content of the drag signal (Figure 10a) dissipates after approximately 1 Hz while the velocity monitor of the wake indicates the presence of strong frequencies up to roughly 2.5 Hz (Fig.10b). As is the case with the 2D simulation, the first 3 modes of the heliostat structure occur around these frequencies.

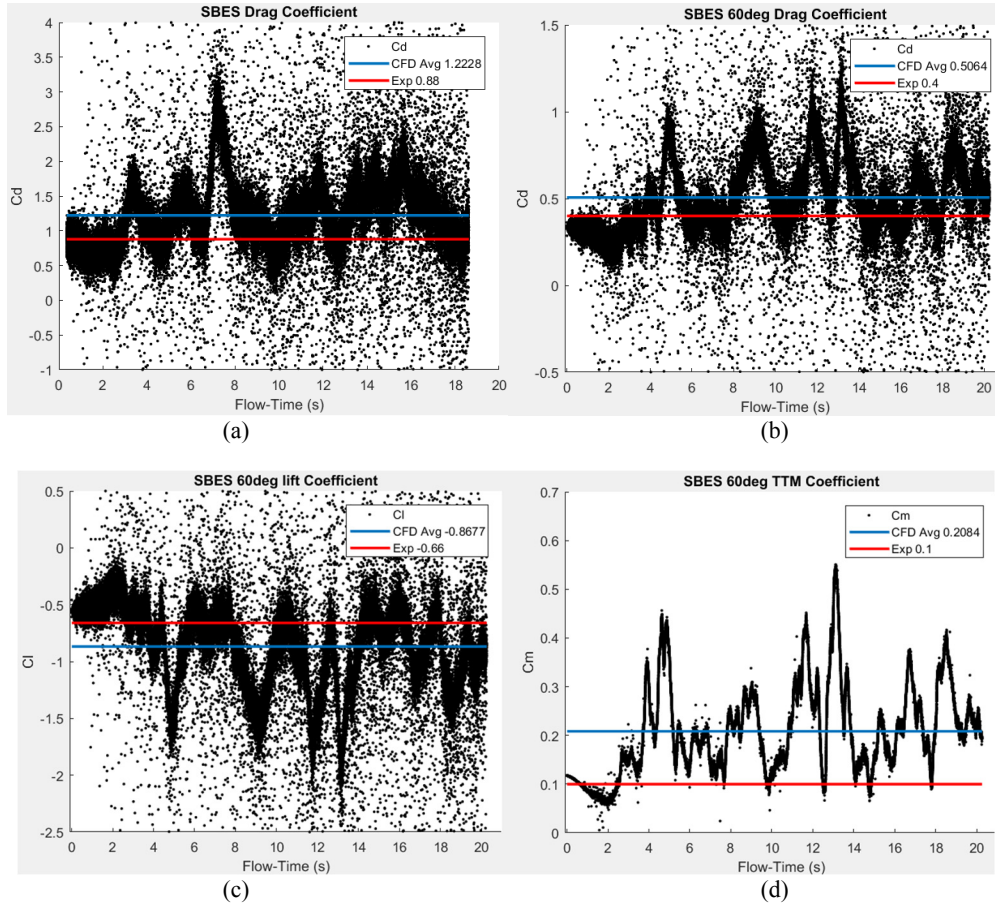
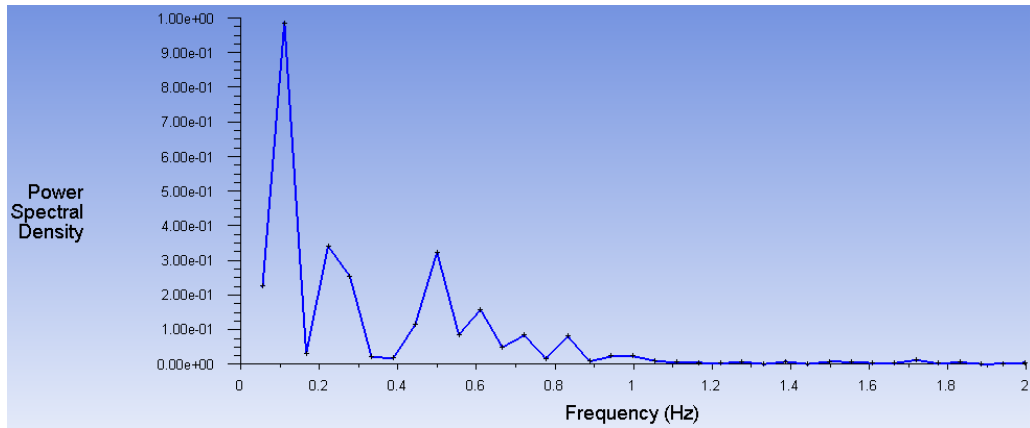
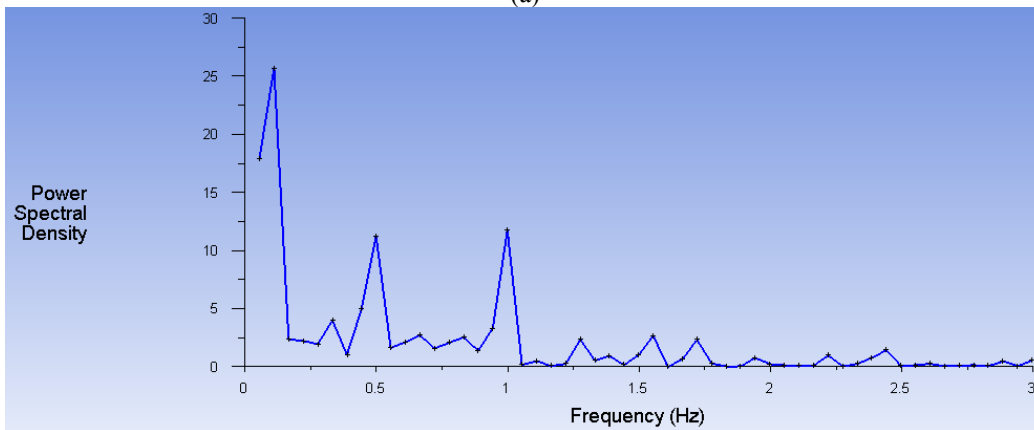


FIGURE 9. Drag coefficient for a) 0° and b) 60° case and c) lift and d) torque tube moment coefficient for 60° SBES as compared to averaged experimental results of Ref.1.

There is a prominent frequency component at 1.73 Hz in the velocity point monitor, that has the ability to resonate the structure, this demonstrates the need to investigate the structural response with the use of one-way FSI. To visualise the turbulent structures that are responsible for the frequency response, iso-surfaces of Q-criterion coloured by velocity magnitude show the coherent structures shed by the heliostat and formed in the wake, (Fig.11a) and b)), with Q-criterion values chosen to highlight the appropriate scales.



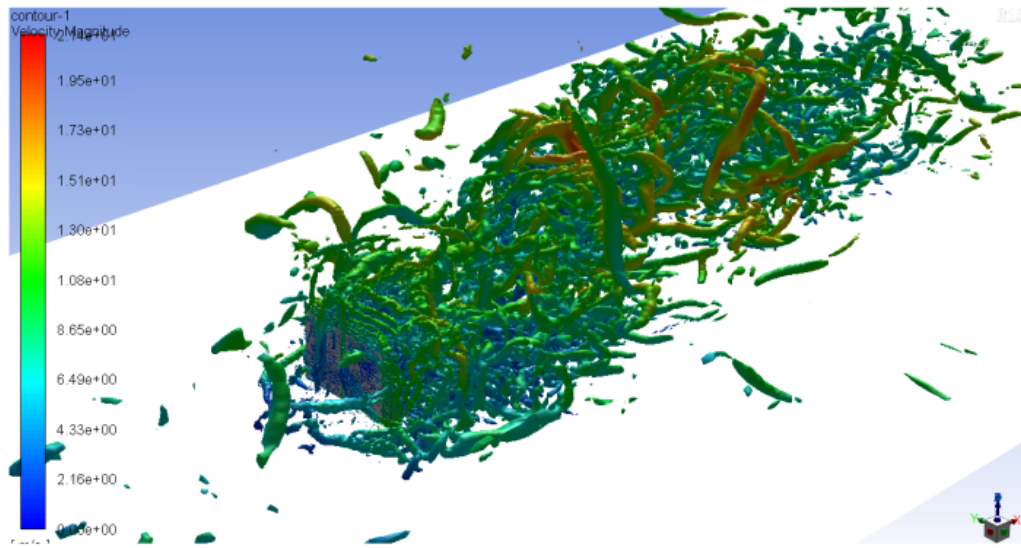
(a)



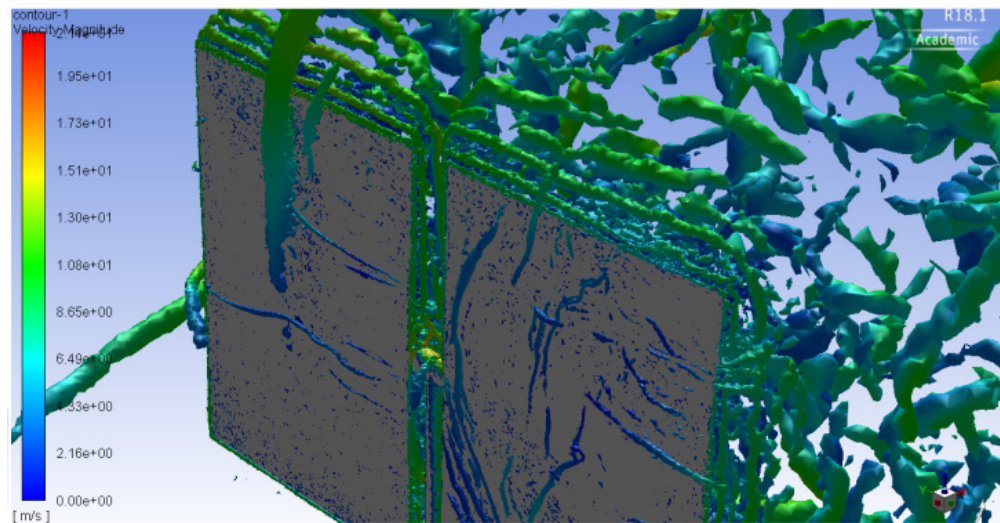
(b)

FIGURE 10. a) Drag coefficient and b) wake velocity point monitor FFTs

The results for the one-way FSI employing the pressure output data calculated using SBES are shown in Figure 12 using 3 seconds of SBES flow time in the developed flow regime. The deformation of the heliostat can be seen as asymmetric as the top right corner of the mirror is seen to be more heavily deformed. Fig.12c) shows the vertex displacement in the flow direction of the top right corner, demonstrating the oscillatory nature of the heliostat when responding to the ABL flow. As yet an FFT of the results has not been conducted, but the dominant frequency in Fig.12c) can be estimated to be around 2.7Hz, implying that the 3rd mode in Fig.7b) could be excited.



(a)



(b)

FIGURE 11. Iso-Surfaces of Q-criterion coloured by velocity magnitude of SBES, a) $Q=100 \text{ s}^{-2}$ b) $Q=1000 \text{ s}^{-2}$

CONCLUSIONS

The 2D URANS simulations of a simplified heliostat geometry appear to offer promising results for the prediction of the vortex shedding frequency. This is an important result as 3D URANS was unable to model any transient behavior in the wake of a geometry such as this, let alone be accurate. There exist several modal frequencies in the range of possible vortex shedding frequencies that could be excited by the wind. The preliminary results of the one-way FSI show that the response of the heliostat to the pressure field derived from the SBES simulation may be of a higher frequency than that of the predicted main vortex shedding frequency. The method demonstrated above for the prediction of vortex shedding from a heliostat and determining the resultant deformation therefore shows promise.

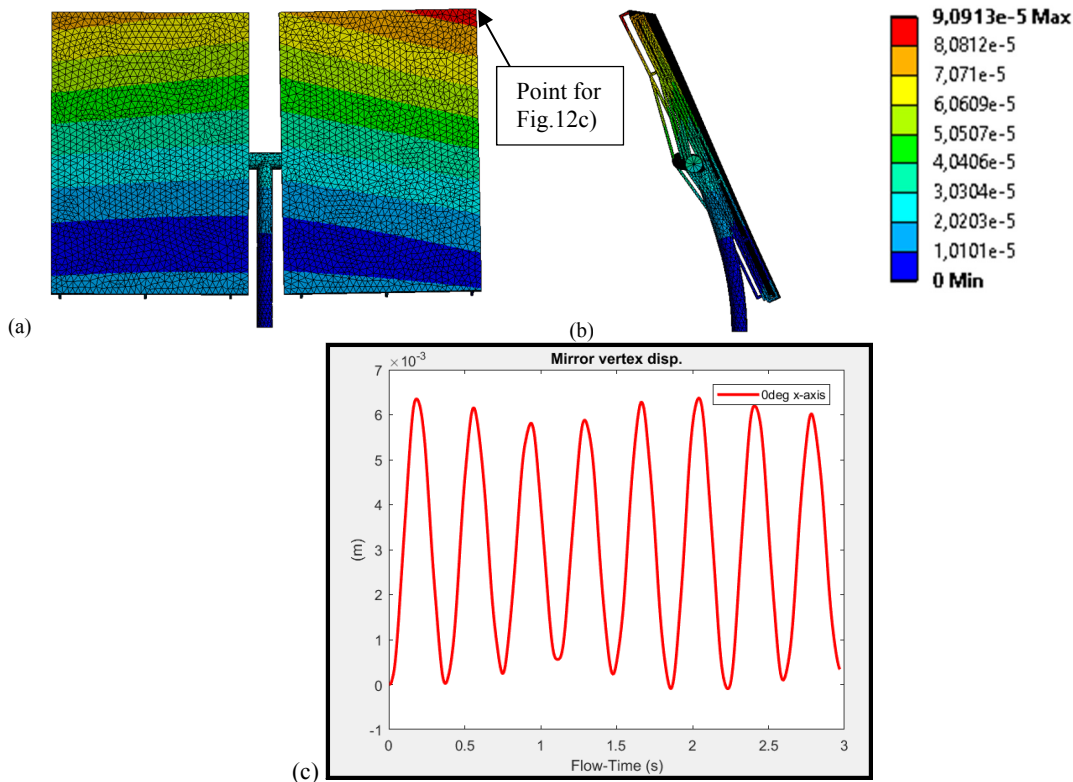


FIGURE 12. a) Total deformation (front) [m] b) Total deformation (side) c) Mirror vertex x-directional displacement [m] history

ACKNOWLEDGEMENTS

The use of the Centre for High Performance Computing (CHPC) in Cape Town, South Africa, is acknowledged.

REFERENCES

1. Huss, S., Traeger, Y. D., Shvets, Z., Rojansky, M., Stoyanoff, S. & Garber, J. Evaluating effects of wind loads in heliostat design. SolarPACES 2011. Granada, Spain: 20–23 September 2011.
2. Sun, H., Gong, B. & Yao, Q. 2014. A review of wind loads on heliostats and trough collectors, [Renewable and Sustainable Energy Reviews](#), 32, 206-221.
3. Blocken, B., Stathopoulos, T. & Carmeliet, J. 2007. CFD simulation of the atmospheric boundary layer: wall function problems. [Atmospheric Environment](#), 41, 238-252.
4. Richards, P. J. & Norris, S. E. 2011. Appropriate boundary conditions for computational wind engineering models revisited. [Journal of Wind Engineering and Industrial Aerodynamics](#), 99, 257-266.
5. Bungartz, H.-J., Schäfer, M. (Eds.), *Fluid-Structure Interaction – Modelling, Simulation, Optimisation*, Springer-Verlag, Berlin, 2006.
6. Matty, R. R. 1979. Vortex shedding from square plates near a ground plane: An experimental study. Masters in Mechanical Engineering, Texas Tech University.
7. Peterka J. A., Hosoya, N., Bienkiewicz, B. & Cermak, J. E. 1986. Wind load reduction for heliostats, Report SERI/STR-253-2859. Golden, Colorado, USA, Solar Energy Research Institute.
8. Griffith, D.T., Moya, A.C., Ho, C.K., Hunter, P.S., Structural Dynamics Testing and Analysis for Design Evaluation and Monitoring of Heliostats, [Journal of Solar Energy Engineering](#), 137 (2015) 021010-1 to 021010-10.